

Subspace based system identification for an acoustic enclosure

Tomas McKelvey *

Dept. of Signals and Systems
Chalmers University of Technology
DE-412 96 Gothenburg, Sweden

Andrew Fleming , **S. O. Reza Moheimani** †

Dept. of Electrical and Computer Eng.
University of Newcastle
Callaghan, NSW 2308, Australia.

December 3, 2001

Abstract

This paper is aimed at identifying a dynamical model for an acoustic enclosure, a duct with rectangular cross section, closed ends, and side mounted speaker enclosures. Acoustic enclosures are known to be resonant systems of high order. In order to design a high performance feedback controller for an acoustic enclosure, one needs to have an accurate model of the system. Subspace based system identification techniques have proven to be an efficient means of identifying dynamics of high order highly resonant systems. In this paper a frequency domain subspace based method together with a second iterative optimization step minimizing a frequency domain least-squares criterion is successfully employed to identify a dynamical model for an acoustic enclosure.

*Supported by the Swedish Foundation for International Cooperation in Research and Higher Education (STINT). This work was completed while the author was visiting Dept. of Electrical and Computer Engineering, University of Newcastle, Australia. The first author holds the position of associate professor.

†The work of the second and third authors was supported by the Australian Research Council and the Center for Integrated Dynamics and Control. The second and third authors hold positions of post graduate student and senior lecturer respectively. All correspondence should be forwarded to the second author.

1 Introduction

During the previous decade there has been a substantial and consistent focus on the problem of active noise cancellation (ANC) in acoustic enclosures and ducts. Early work concentrated mainly on adaptive feedforward configurations such as those detailed in [8]. Such techniques involve the measurement of a disturbance and attempt to arrest the propagation downstream. Although impressive results have been achieved for ducts with end mounted disturbances (see for example [17, 18]) new approaches have been required to confront the greater problems of multiple disturbances, three dimensional sound fields, and spatial cancellation. More recent work involves the design of feedback control systems to cancel or absorb noise in acoustic enclosures, see, e.g., [1, 15, 16].

Model-based feedback control strategies require a reliable model of the system that is to be controlled. Various authors have addressed the problem of analytic modeling of ducts and enclosures, see, e.g., [5, 2, 4]. It is known however, that analytic modeling may result in a poor model if the system is even mildly realistic (see reference [4]). System identification methods may be employed for this purpose. Such methods are convenient as they model the overall system, i.e. the acoustic dynamics of the duct in addition to exterior systems such as actuator dynamics, amplifiers, and filters. To obtain an analytical model, all of these items have to be modeled separately, then combined to construct the overall system.

Methods which identify state-space models by means of geometrical properties of the input and output sequences are commonly known as subspace methods. These methods have received much attention in the literature (see [22] for a survey of time domain techniques). One of the advantages of subspace methods is that an estimate is calculated without any non-linear parametric optimization over the entire model space. In classical prediction error minimization [10], such a step is necessary for most model structures. A second advantage is that the identification of multivariable systems is just as simple as that of scalar systems. This may prove an important advantage for ANC applications where a large number of actuators and sensors are used.

In this paper we consider the case where data is given in the frequency domain, i.e. when samples of the Fourier transform of the input and output signals are taken as the primary measurements. In a number of applications, particularly when modeling flexible structures, it is common to fit models in the frequency domain [19, 14]. A few subspace based algorithms formulated in the frequency domain have appeared recently [9, 12, 20, 11]

From a statistical point of view it is well known that, under some assumptions, the best models are obtained by the method of maximum-likelihood. In this paper

we will, as a second step, after obtaining an initial model from the subspace method, invoke a parametric optimization minimizing the 2-norm of the frequency domain error. Under suitable assumptions this can be interpreted as a maximum-likelihood estimation step [14]. It is important to point out that the success of the second parametric optimization is heavily based on the availability of a good starting point for the optimization.

1.1 Preliminaries

Consider a stable time-invariant discrete time linear system of finite order n in state-space form

$$\begin{aligned}x(k+1) &= Ax(k) + Bu(k) \\ y(k) &= Cx(k) + Du(k) + v(k)\end{aligned}\tag{1}$$

where $u(k) \in \mathbb{R}^m$ is the input vector, $y(k) \in \mathbb{R}^p$ the output vector and $x(k) \in \mathbb{R}^n$ is the state vector. By considering real valued signals we implicitly assume that the matrix quadruple (A, B, C, D) is also real valued. The noise term $v(k) \in \mathbb{R}^p$ is assumed to be independent of the input sequence $u(k)$. Here the time index k denotes normalized time. Hence $y(k)$ denotes the sample of the output signal $y(t)$ at time instant $t = kT_s$ where T_s denotes the sample time. We also assume that the state-space realization (1) is minimal which implies both observability and controllability [7]. A system with this type of noise model is commonly known as output-error models [10]. Note that all such pairs (1) describing the same input/output behavior of the system are equivalent under a non-singular similarity transformation $T \in \mathbb{R}^{n \times n}$ [7], *i.e.* the matrices $(T^{-1}AT, T^{-1}B, CT, D)$ will be a state-space realization with equivalent i/o properties.

The discrete time Fourier transform \mathcal{F} of a sequence $f(k)$ is defined as

$$\mathcal{F}f(k) = F(\omega) = \sum_{k=-\infty}^{\infty} f(k)e^{-j\omega k}\tag{2}$$

where $j = \sqrt{-1}$. Applying the Fourier transform to (1) gives

$$\begin{aligned}e^{j\omega}X(\omega) &= AX(\omega) + BU(\omega) \\ Y(\omega) &= CX(\omega) + DU(\omega) + V(\omega)\end{aligned}\tag{3}$$

where $Y(\omega), U(\omega), V(\omega)$ and $X(\omega)$ are the transformed output, input, noise and state respectively. By eliminating the state from (3) we obtain

$$Y(\omega) = G(e^{j\omega})U(\omega) + V(\omega)\tag{4}$$

where $G(z) = D + C(zI - A)^{-1}B$ is known as the transfer function of the linear system.

1.2 The Identification Problem

Given samples of the discrete time Fourier transform of the input signal $U(\omega)$ and output signal $Y(\omega)$ at N arbitrary frequency points ω_k ; find a state-space model of the form (1) which well approximates the data in a least-squares fashion, i.e.

$$\hat{G}(z) = \arg \min_{G(z)} \sum_{k=1}^N \|Y(\omega_k) - G(e^{j\omega_k})U(\omega_k)\|^2 \quad (5)$$

2 Identification method

This section is devoted to describing the identification technique used. As a first step a state-space model is identified using a frequency domain subspace based algorithm. The identified state-space realization is then transformed to a tridiagonal realization suitable for a tridiagonal parameterization. Finally an optimization is employed to minimize the 2-norm of the identification error system (see (5)). Here the tridiagonal parameterization and an iterative Gauss-Newton non-linear least-squares algorithm is utilized to find a (local) optimum of the least-squares criterion function.

2.1 Frequency domain subspace method

In this section we will outline the basic relations that characterize the frequency domain subspace identification problem. Let us introduce the vector

$$W(\omega) = \left[1 \quad e^{j\omega} \quad e^{j2\omega} \quad \dots \quad e^{j\omega(q-1)} \right]^T \quad (6)$$

the extended observability matrix with q block rows

$$\mathcal{O}_q = \begin{bmatrix} C \\ CA \\ \vdots \\ CA^{q-1} \end{bmatrix} \quad (7)$$

and the lower triangular Toeplitz matrix

$$\Gamma_q = \begin{bmatrix} D & 0 & \dots & 0 \\ CB & D & \dots & 0 \\ \vdots & \vdots & \ddots & \vdots \\ CA^{q-2}B & CA^{q-3}B & \dots & D \end{bmatrix} \quad (8)$$

By recursive use of (3) we obtain

$$\begin{aligned} W(\omega) \otimes Y(\omega) &= \mathcal{O}_q X(\omega) + \Gamma_q W(\omega) \otimes U(\omega) \\ &\quad + W(\omega) \otimes V(\omega) \end{aligned} \quad (9)$$

where \otimes denotes the standard Kronecker product [7]. The extended observability matrix \mathcal{O}_q has a rank equal to the system order n if $q \geq n$ since the system (A, B, C, D) is minimal.

If N samples of the transforms are known we can collect all data into one complex matrix equation. Define the diagonalization operator for a sequence of vectors z_i of length p as

$$\text{diag}[z_1, z_2, \dots, z_N] \triangleq \begin{bmatrix} z_1 & 0 & & 0 \\ 0 & z_2 & \ddots & \\ & \ddots & \ddots & \\ 0 & & 0 & z_N \end{bmatrix} \quad (10)$$

which is a tall (or square) matrix of size $Np \times N$. By introducing the additional matrices

$$\begin{aligned} \mathbf{W}_{N,p} &= \begin{bmatrix} W(\omega_1) & W(\omega_2) & \cdots & W(\omega_N) \end{bmatrix} \otimes I_p \\ \mathbf{Y}^c &= \frac{1}{\sqrt{N}} \mathbf{W}_{N,p} \text{diag}[Y(\omega_1), \dots, Y(\omega_N)] \in \mathbb{C}^{qp \times N}, \\ \mathbf{U}^c &= \frac{1}{\sqrt{N}} \mathbf{W}_{N,m} \text{diag}[U(\omega_1), \dots, U(\omega_N)] \in \mathbb{C}^{qm \times N}, \\ \mathbf{V}^c &= \frac{1}{\sqrt{N}} \mathbf{W}_{N,p} \text{diag}[V(\omega_1), \dots, V(\omega_N)] \in \mathbb{C}^{qp \times N}, \\ \mathbf{X}^c &= \frac{1}{\sqrt{N}} \begin{bmatrix} X(\omega_1), & \cdots, & X(\omega_N), \end{bmatrix} \in \mathbb{C}^{n \times N}, \end{aligned}$$

and using (9) we arrive at the matrix equation

$$\mathbf{Y}^c = \mathcal{O}_q \mathbf{X}^c + \Gamma_q \mathbf{U}^c + \mathbf{V}^c. \quad (11)$$

The superscript c is used to stress that the matrix is complex valued. Clearly since the system matrices are assumed real valued \mathcal{O}_q and Γ_q are also real. Hence by forming a real matrix from the real and complex parts of \mathbf{Y}^c as

$$\mathbf{Y} = \begin{bmatrix} \text{Re}\{\mathbf{Y}^c\} & \text{Im}\{\mathbf{Y}^c\} \end{bmatrix}$$

and similarly for $\mathbf{U}, \mathbf{X}, \mathbf{V}$ we obtain the real valued matrix equation

$$\mathbf{Y} = \mathcal{O}_q \mathbf{X} + \Gamma_q \mathbf{U} + \mathbf{V}. \quad (12)$$

Note that this equation now has $2N$ columns. As the number of frequency samples increases the number of columns in the matrix equation (12) also increases. The

normalization with $\frac{1}{\sqrt{N}}$ ensures that the norm of the matrix stays bounded as the number of frequencies (columns) tends to infinity. The number of (block)-rows q is up to the user to choose but must be larger than the upper bound of the model orders which will be considered.

The identification scheme we employ to find a state-space model $(\hat{A}, \hat{B}, \hat{C}, \hat{D})$ is based on a two step procedure. First the relation (12) is used to consistently determine a matrix $\hat{\mathcal{O}}_q$ with a range space equal to the extended observability matrix \mathcal{O}_q . From $\hat{\mathcal{O}}_q$ it is straightforward to derive \hat{A} and \hat{C} as is well known from the time domain subspace methods [22]. In the second step \hat{B} and \hat{D} are determined by performing a well known linear regression using the previously determined matrices and frequency response [12].

2.2 The Basic Projection Method

The first step of the subspace method aims at providing an estimate of the range space of the observability matrix $\hat{\mathcal{O}}_q$. First consider the noise free case $\mathbf{V}_{q,N} = 0$ and we restate the basic projection method [22] in the frequency domain. In (12) the term $\Gamma_q \mathbf{U}$ can be removed by a projection. Denote by Π^\perp the orthogonal projection onto the null-space of \mathbf{U} ,

$$\Pi^\perp = I - \mathbf{U}^T(\mathbf{U}\mathbf{U}^T)^{-1}\mathbf{U} \quad (13)$$

here \mathbf{U}^T denotes the transpose of the matrix \mathbf{U} . The inverse in (13) will exist if the input is sufficiently rich. See [12] for details. Since $\mathbf{U}\Pi^\perp = 0$ the effect of the input will be removed and we obtain $\mathbf{Y}\Pi^\perp = \mathcal{O}_q\mathbf{X}\Pi^\perp$. Provided $\text{rank}(\mathbf{X}\Pi^\perp) = n$. $\mathbf{Y}\Pi^\perp$ and \mathcal{O}_q will span the same column space. The mild conditions required for the previous relation to hold can be found in [12].

A matrix which concisely spans the column space of $\mathbf{Y}_{q,N}\Pi^\perp$ can be recovered in a singular value decomposition [6]

$$\mathbf{Y}\Pi^\perp = \begin{bmatrix} U_s & U_o \end{bmatrix} \begin{bmatrix} \Sigma_s & 0 \\ 0 & \Sigma_o \end{bmatrix} \begin{bmatrix} V_s^T \\ V_o^T \end{bmatrix} \quad (14)$$

where $U_s \in \mathbb{R}^{q \times n}$ contains the n left principal singular vectors and the diagonal matrix Σ_s the corresponding singular values. In the noise free case $\Sigma_o = 0$ and there will exist a nonsingular matrix $T \in \mathbb{R}^{n \times n}$ such that $\mathcal{O}_q = U_s T$. This shows that U_s is an extended observability matrix $\hat{\mathcal{O}}_q$ of the original transfer function for some realization. By the shift structure of the observability matrix (7) we can proceed to calculate A and C as

$$\hat{A} = \arg \min_A \|J_1 U_s A - J_2 U_s\|_F^2 = (J_1 U_s)^\dagger J_2 U_s \quad (15)$$

$$\hat{C} = J_3 U_s \quad (16)$$

where J_i are the selection matrices defined by

$$J_1 = \begin{pmatrix} I_{(q-1)p} & 0_{(q-1)p \times p} \end{pmatrix}, \quad (17)$$

$$J_2 = \begin{pmatrix} 0_{(q-1)p \times p} & I_{(q-1)p} \end{pmatrix}, \quad (18)$$

$$J_3 = \begin{pmatrix} I_p & 0_{p \times (q-1)p} \end{pmatrix} \quad (19)$$

and I_i denotes the $i \times i$ identity matrix, $0_{i \times j}$ denotes the $i \times j$ zero matrix, $\|\cdot\|_F$ is the Frobenius norm and $X^\dagger = (X^T X)^{-1} X^T$ denotes the Moore-Penrose pseudo-inverse of the full rank matrix X . With the knowledge of \hat{A} and \hat{C} , we can now calculate estimates for \hat{B} and \hat{D} [12]. The reader is referred to [12] for an efficient method of forming $Y\Pi^\perp$ using QR factorization.

2.3 Consistency Issues

As we have seen, the basic projection algorithm will estimate a state-space model that is similar to the original realization in the noise free case. If the noise term $V(\omega)$ is a zero mean complex random variable the issue of consistency becomes important. Does the estimate converge to the true system as N , the number of data, tends to infinity? Consistency of the basic projection algorithm and the related algorithm [9] has been investigated in [12, 20]. The result is that unless the covariance structure of the data is known, consistency cannot be expected. Results describing the asymptotic variance for an unknown noise model can be found in [14]. For the application studied in this paper, due to a high SNR, the basic projection method produces sufficiently good estimates although the noise structure is unknown. A second approach based on the classical instrumental variable technique (IV) [10] does not require knowledge of the variance properties (or equivalently the color of the noise). Subspace based time IV-techniques can be found in [21]. A frequency domain subspace-IV-approach can be found in [11].

2.4 Non-linear optimization

The initial estimate delivered by the subspace method is a good starting point for a non-linear iterative optimization of the desired criterion (5). The optimization is assumed to be quasi-convex in the region of the initial estimate. For high order systems, a numerically sound parameterization of the transfer function $G(z)$ is required. A parameterization based on the state-space form (1) using a tridiagonal A matrix has recently been suggested [13]. Particularly the tridiagonal parameterization has

shown promising numerical properties for high order systems. Let

$$G(z, \theta) = D(\theta) + C(\theta)(zI - A(\theta))^{-1}B(\theta) \quad (20)$$

be a transfer function parameterized through the state-space matrices by the real valued vector θ using the tridiagonal model structure. A Gauss-Newton algorithm [3] is employed for finding a solution to the parametric optimization problem

$$\hat{\theta} = \arg \min_{\theta} \sum_{k=1}^N \|Y(\omega_k) - G(e^{j\omega_k}, \theta)U(\omega_k)\|^2 \quad (21)$$

The optimization algorithm is started from the parameter vector θ_0 representing the transfer function delivered by the subspace method. For high order systems it is vital to have a high quality starting point in order to converge to a good optimum. Since the Gauss-Newton algorithm only converges locally to a minimum a starting point close to the global optimum is desirable. If we assume the frequency domain noise is complex Gaussian and white the solution to (21) will be the maximum-likelihood estimate [14].

3 The Experiment

The experiment was conducted in the Laboratory for Dynamics and Control of Smart Structures at the University of Newcastle, Australia. A plan view of the acoustic duct apparatus is shown in Figure 1, while the actual setup can be seen in Figure 2. For disturbance rejection a feedback loop is to be closed around the control speaker to microphone path. This path represents a system where the speaker signal and microphone voltage are the input and output respectively. The system dynamics consists of a series combination of the following transfer functions: speaker signal low pass filter, power amplifier, applied speaker voltage to baffle acceleration, baffle acceleration to sound pressure, and the gain of the microphone from sound pressure to voltage.

Speaker 2 is used in control system experimentation and is redundant during identification. Our ultimate goal is to use this setup for ANC experiments, which will be reported subsequently. However, for the moment, the second speaker is not used. Although it is unused, this speaker must remain attached. This is due to the coupling that exists between the passive dynamics of the speaker and the enclosed sound field. For a discussion of the coupling between passive speaker dynamics and enclosed sound fields the reader is referred to [2].

The acoustic actuators are constructed from 10 inch diameter speakers (Jaycar CS-2220) and a sealed enclosure of 23 liters. The main reason for this arrangement

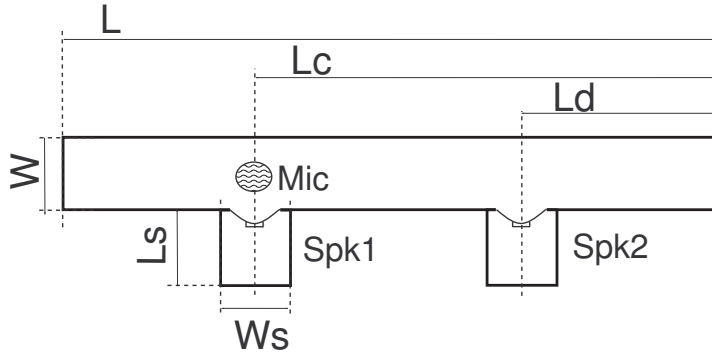


Figure 1: Plan view of the acoustic duct apparatus.



Figure 2: The experimental acoustic enclosure.

is to improve the low frequency dynamics of the speakers. The frequency response between applied voltage and baffle acceleration was measured to determine a low frequency bandwidth of 55 Hz. The measurement was taken using a Polytec scanning laser vibrometer (PSV-300) and is shown in Figure 3. If an analytic model of the system is to be derived, one would need to fit a model to the measured data shown in Figure 3. This model would then be combined with the duct dynamics as explained in [5]. However, since we employ a system identification method to model the dynamics of the whole system, we may simply skip this step.

The acoustic sensor is a unidirectional dynamic microphone (Schure SM58) with a bandwidth of 50 to 15,000 Hz and a pressure sensitivity of -56 dB ($0 \text{ dB} = 1\text{V}/\mu\text{bar}$). This is a suitable sensor for this apparatus since the low cut-off frequency of the actuator is also, roughly, 50 Hz.

The excitation signal generation and data recording is performed using the dSPACE-DS1103 rapid prototyping system. The excitation signal is a uniformly distributed random process sampled at 2 kHz and digitally filtered with a 6th order

Dimension	Value
L	4.840 m
Ls	0.320 m
Lc	2.940 m
Ld	0.940 m
W	0.246 m
Ws	0.246 m
Height	0.295 m

Table 1: Duct Internal Dimensions

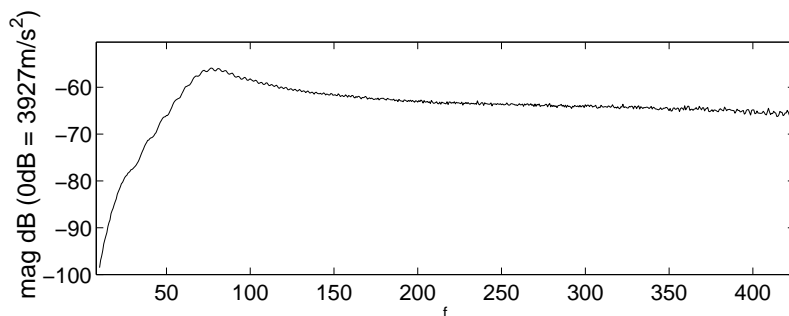


Figure 3: Magnitude response of the acoustic actuators from applied voltage to baffle acceleration

elliptic bandpass filter between 50 and 400 Hz. The DAC output is filtered with a 1 kHz analog low pass filter to remove the sampling frequency component and harmonics. The microphone signal is filtered using low-pass 1 kHz 4th order anti-aliasing filters and is recorded at 2 kHz with 16 bit resolution for 60 seconds. The filter used in this experiment is a Frequency Devices 9002 Dual channel programmable switched capacitor filter.

4 Identification results

The experimental input-output time series is divided into two equal size data sets, one estimation set and another set for validation purposes. The estimation data is transformed to the frequency domain by use of the fast Fourier transform (FFT) without any windowing functions. As the frequency content of the excitation signal is restricted to the 50-400 Hz frequency band all frequency data outside this interval is discarded. This reduces the size of the data sets to 5456 samples. As the input to the system is based on a filtered random signal the spectrum of the input fluctuates over the frequencies. In order to only use highly excited frequencies, only frequency

points with an input amplitude above 1.7 are retained in the identification set. This leads to an identification set with 1545 points with a high SNR. The subspace estimation algorithm outlined in Section 2 is employed to estimate a model of order 29 using $q = 60$ as the number of rows in the matrix equation (12).

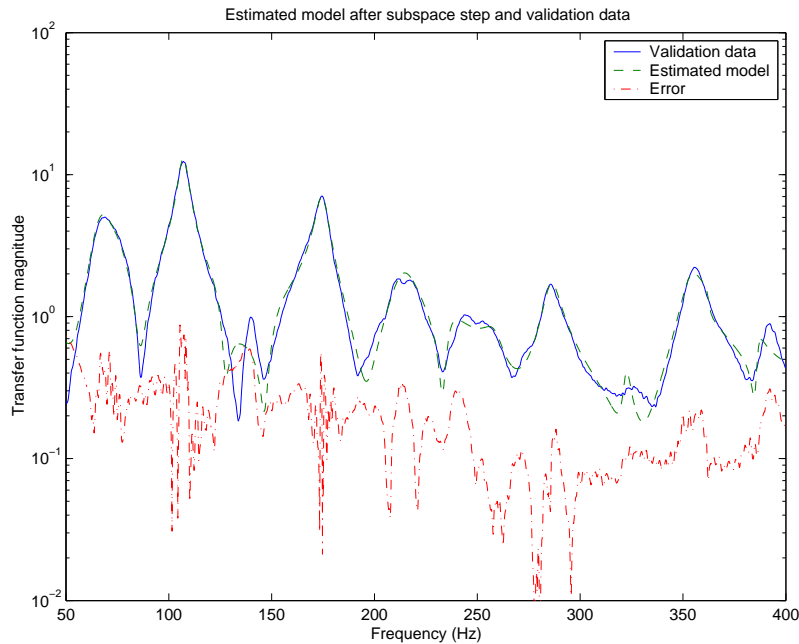


Figure 4: Magnitude transfer functions of parametric model estimate of order 29 from subspace algorithm and ETFE from validation data. The magnitude of the error also is shown. The transfer functions are derived from the applied actuator voltage to measured microphone preamp voltage. (-) Validation Data, (- -) Estimated model, (- -) Error.

To validate the model, or rather to check if there is any evidence in the data which implies that the model is *invalid*, we use an independent validation data set of 31178 samples to derive the Empirical Transfer Function Estimate (ETFE) [10] of the system. In particular the ETFE is calculated at $N_v = 2^{13} = 8192$ frequency points equally spaced between 0 and 1kHz. The ETFE is the fraction between the cross spectrum between the input and output and the auto spectrum of the input.

$$\hat{H}(\omega) = \frac{\hat{\Phi}_{yu}(\omega)}{\hat{\Phi}_{uu}(\omega)} \quad (22)$$

In the calculation of the spectral estimates $\hat{\Phi}_{yu}(\omega)$ and $\hat{\Phi}_{uu}(\omega)$ a Hamming window of size 1024 is employed to smooth the estimates.

The transfer functions of the subspace estimate and the ETFE are plotted together in Figure 4. The RMS error between the parametric model \hat{G} and the vali-

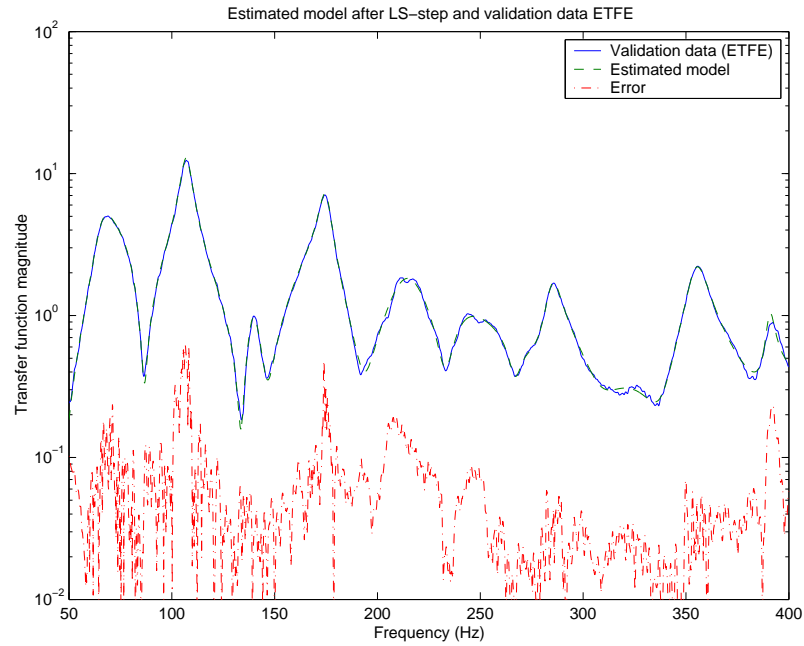


Figure 5: Final estimated model after parametric optimization of LS criterion. Magnitude and error plot showing estimated model of order 29 and ETFE from validation data. The transfer functions are derived from the applied actuator voltage to measured microphone preamp voltage. (-) Validation Data, (- -) Estimated model, (- -) Error.

dition ETFE \hat{H} is 0.24. The RMS error is defined as

$$\text{RMS} = \sqrt{\frac{1}{2867} \sum_{k \in \mathcal{V}} \left\| \hat{H}(\omega_k) - \hat{G}(e^{j\omega_k}) \right\|^2} \quad (23)$$

where \mathcal{V} denote the set of frequency indices k corresponding to the frequency band 50-400 Hz and consists of 2867 elements.

The nonlinear optimization step further improved the RMS error to a value of 0.09 again calculated against the validation data ETFE. The amplitude of the finally estimated transfer function is depicted in Figure 5 together with the validation data ETFE. Also the magnitude of the complex error between the estimated model and the validation data is shown in the figure.

As a second validation step a time domain simulation comparing the output of the model to the time domain validation output is performed. The validation input is used to simulate the output of the 29th order model. An excerpt of the simulation is shown in Figure 6. The output of the model is almost identical to the measured output of the validation data.

The estimated model is implemented in the dSPACE DSP prototype equipment and used to predict the sound pressure at the microphone position in real-time. The load speaker is driven with a disturbance signal, the addition of 50-400 Hz random noise and a sinusoid at 71 Hz (near the first mode). The output is measured using the microphone, and a prediction is produced by simulating the 29th order model in real time. An excerpt from the measured and predicted data is shown in Figure 7.

Based on the cross validation both in the frequency domain as well as the time domain it can be concluded that the estimated model is quite accurate. Hence the model should be a good candidate for use in a model based control design although bearing in mind the level of estimation error or uncertainty as indicated by the error curve in Figure 5.

5 Conclusions

In this paper we successfully identified a dynamical model for an acoustic enclosure. Firstly an initial model of the system was estimated using a frequency domain subspace based identification algorithm. In a second step the estimate was refined by minimizing the 2-norm of the frequency error between the model and data. This was achieved using a tridiagonal parameterization of a state-space model utilizing a Gauss-Newton type optimization algorithm. The quality of the estimated model was assessed in both time and frequency domain using independent validation data. The result indicates that the model is accurate over the frequency range of interest, and is suitable for high performance model based control design techniques.

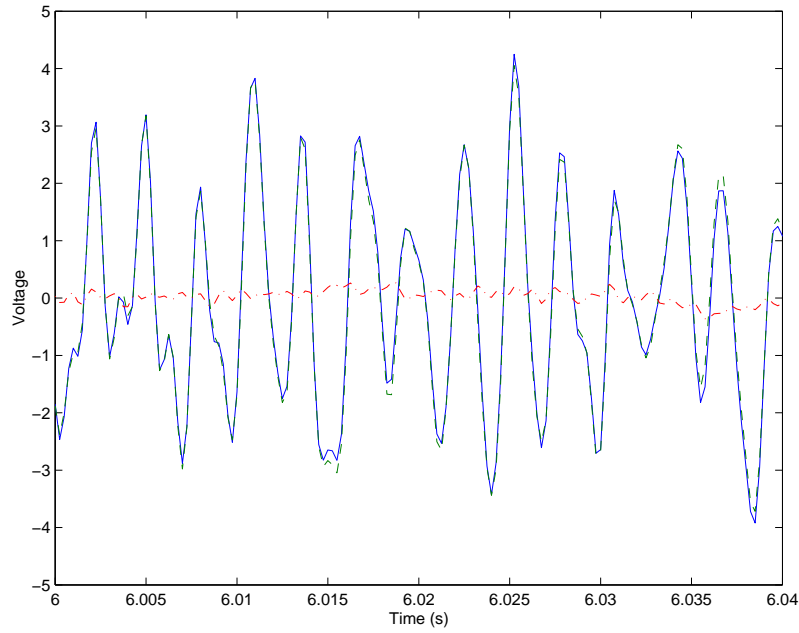


Figure 6: Time domain comparison between the simulated output of the estimated model and the measured output. The input and outputs are taken as the applied actuator voltage and microphone preamp voltage. (-) Validation Data, (- -) Estimated model, (- -) Error.

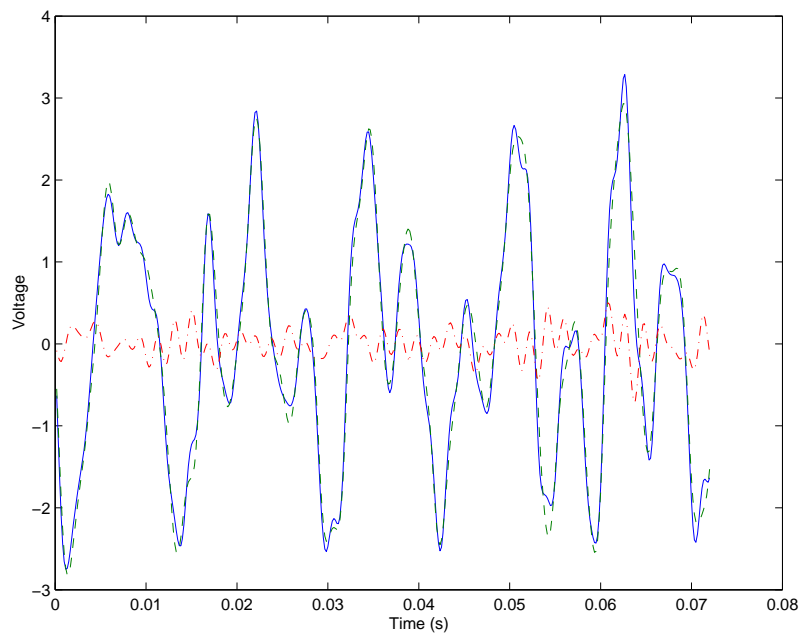


Figure 7: Result from a real-time validation experiment comparing the simulated output of the estimated model and the measured output of the system. The input and outputs are taken as the applied actuator voltage and microphone preamp voltage. (-) Real time measurement, (- -) Estimated model, (- -) Error.

References

- [1] S. C. Southward A. J. Hull, C. J. Radcliffe. Global active noise control of a one dimensional acoustic duct using a feedback controller. *Transactions of the ASME, Journal of Dynamic Systems Measurements and Control*, 115:488–494, sep 1993.
- [2] R. L. Clark and K. D. Frampton. Phase compensation for feedback control of enclosed sound fields. *Journal of Sound and Vibration*, 195(5):701–, 1985.
- [3] J. E. Dennis and R. B. Schnabel. *Numerical Methods for Unconstrained Optimization and Nonlinear Equations*. Prentice-Hall, Englewood Cliffs, New Jersey, 1983.
- [4] A. G. Kelkar H. R. Pota. Modelling, identification, and control of acoustic ducts. preprint, 2000.
- [5] J. Hong, J. C. Akers, R. Venugopal, M. Lee, A. G. Sparks, P. D. Washabaugh, and D. Bernstein. Modeling, identification, and feedback control of noise in an acoustic duct. *IEEE Tran, on Control Systems Technology*, 4(3):283–291, May 1996.
- [6] R. A. Horn and C. R. Johnson. *Matrix Analysis*. Cambridge University Press, Cambridge, NY, 1985.
- [7] T. Kailath. *Linear Systems*. Prentice-Hall, Englewood Cliffs, New Jersey, 1980.
- [8] S. M. Kuo and D. R. Morgan. *Active noise control system*. John Wiley and Sons Inc., 1996.
- [9] K. Liu, R. N. Jacques, and D. W. Miller. Frequency domain structural system identification by observability range space extraction. In *Proc. American Control Conference, Baltimore, Maryland*, volume 1, pages 107–111, June 1994.
- [10] L. Ljung. *System Identification: Theory for the User*. Prentice-Hall, Englewood Cliffs, New Jersey, 1987.
- [11] T. McKelvey. Frequency domain system identification with instrumental variable based subspace algorithm. In *Proc. 16th Biennial Conference on Mechanical Vibration and Noise, DETC'97, ASME*, pages VIB–4252, Sacramento, California, USA, September 1997.
- [12] T. McKelvey, H. Akçay, and L. Ljung. Subspace-based multivariable system identification from frequency response data. *IEEE Trans. on Automatic Control*, 41(7):960–979, July 1996.

- [13] T. McKelvey and A. Helmersson. State-space parametrizations of multivariable linear systems using tridiagonal matrix forms. In *Proc. 35th IEEE Conference on Decision and Control*, pages 3654–3659, Kobe, Japan, December 1996.
- [14] T. McKelvey and L. Ljung. Frequency domain maximum likelihood identification. In *Proc. of the 11th IFAC Symposium on System Identification*, volume 4, pages 1741–1746, Fukuoka, Japan, July 1997.
- [15] P. Mehta, Y. Zheng, C. V. Hollot, and Y. Chait. Active noise control in ducts: Feedforward/feedback design by blending \mathcal{H}_∞ and QFT methods. In *Proc. 13th IFAC World Congress*, pages 191–197, San Francisco, CA, 1996.
- [16] K. A. Morris. Noise reduction in ducts achievable by point control. *ASME Journal of Dynamics Systems, Measurement and Control*, 120:216–223, 1998.
- [17] C. F. Ross. Demonstration of active control of broadband noise. *Journal of Sound and Vibration*, 74(3):411–, 1981.
- [18] A. Roure. Self-adaptive broadband active sound control system. *Journal of Sound and Vibration*, 101(3):429, 1985.
- [19] J. Schoukens and R. Pintelon. *Identification of Linear Systems: a Practical Guideline to Accurate Modeling*. Pergamon Press, London, UK, 1991.
- [20] P. Van Overschee and B. De Moor. Continuous-time frequency domain subspace system identification. *Signal Processing, EURASIP*, 52(2):179–194, July 1996.
- [21] M. Verhaegen. Subspace model identification, Part III: Analysis of the ordinary output-error state space model identification algorithm. *Int. J. Control*, 58:555–586, 1993.
- [22] M. Viberg. Subspace-based methods for the identification of linear time-invariant systems. *Automatica*, 31(12):1835–1851, 1995.